Modification of power characteristics in an array of floating wave energy devices

B. F. M. Child[1] and V. Venugopal[1]

[1]Institute for Energy Systems,
School of Engineering,
The University of Edinburgh,
Edinburgh, EH9 3JL, UK.
E-mail: benjamin.child@ed.ac.uk
E-mail: v.venugopal@ed.ac.uk

Abstract

In this paper we seek configurations of wave energy devices that help to achieve certain objectives, such as maximising power for a given sea state. Preliminary results from a genetic algorithm optimisation and a new heuristic array construction method are presented. These procedures employ an exact hydrodynamic interaction technique, which is used to assess the performance of the resulting arrays. The power enhancing effect of the arrangement ($\bar{q}$-factor) is presented for regular incident waves with a range of frequencies and directions. Finally we evaluate how effective the two optimisation approaches are in achieving the desired modifications to the collective behaviour of devices.

Keywords: Array, Linear wave theory, Genetic algorithm

1 Introduction

An increasing number of developers and researchers are now giving serious consideration not only to wave energy device design but also to the practicalities of deploying many devices together in a wave farm. Careful analysis of these multiple installations is needed since the associated hydrodynamic interactions may be beneficial or indeed harmful to the performance of the array as a whole. The matter is further complicated by the fact that there are several qualities of collective device behaviour that may be desirable (including, but not limited to, maximising total power output for a given wavelength or ensuring the array performs well in a wide range of sea states). Since the configuration of wave energy devices within an array can have a significant impact on many of these, we turn our attention in this paper to seeking arrangements of converters with potentially desirable characteristics.

Fitzgerald and Thomas [1] presented some preliminary results on arrays designed to maximise power output at a certain wave frequency, using the 'point absorber' approximation, whereby the influence of diffracted waves is neglected. However, there are a number of realistic scenarios where this fails, including the analysis of devices which themselves consist of many closely spaced absorbers. It is therefore desirable to include the effects of device scattering in the computations. If the converter is modelled as a truncated vertical cylinder, we may apply the theory of Garrett [2] who solved the diffraction problem using linear wave theory. The interaction method of Kagemoto and Yue [3] may then be used to link together individual solutions, as was done by Yilmaz [4] for a group of cylinders that may also move and radiate waves in synchrony. This work has been extended by the authors [5] to allow for independent movement of bodies in the heave direction and includes the additional capacity to calculate power from the array. The method has since been used to investigate several array configurations and relate some of their geometrical features to characteristics of the array behaviour [6].

In this paper we will attempt to find and analyse arrays of devices that solve the following three problems:

1. **Maximal Array of Real Tuned Devices.** *Given that the converters have been tuned to a particular wave number by selecting only the damping coefficient of the power take-off, find an array configuration which maximises total power production at the same frequency.* This involves the simplest type of device that only needs to be capable of channeling energy in one direction. Also, since resonance is not enforced at the tuning frequency, motion responses are small and the solution here exhibits scattered waves dominating over radiated ones.

2. **Maximal Array of Reactively Tuned Devices.** *Given that the converters have been tuned to a particular wave number by selecting both the spring and damping coefficients of the power take-off, find an array configuration which maximises to-*

tal power production at the same frequency. This case is designed to produce the strongest interactions and the largest power enhancement. However, results near resonance should be treated with caution, since the large amplitudes of motion may well violate the assumptions of linear wave theory.

3. **Minimal Array of Reactively Tuned Devices.** *Given that the converters have been tuned to a particular wave number by selecting both the spring and damping coefficients of the power take-off, find an array configuration which minimises total power production at the same frequency.* Since the peak isolated device power may not be practically attainable, we may wish to focus instead on broadening the response of the array to different incident wave frequencies [7]. The spatial periodicity of incoming waves leads to oscillations in the nature of interference throughout the frequency range [6], so reducing output at the resonant frequency may lead to increased power for higher and lower wave numbers. This case will also demonstrate the capability of hydrodynamic interactions to diminish as well as enhance power output.

The tuning of the spring and damping constants is sub-optimal, in that power is only optimised for one wave frequency and direction. This is necessary since it is impossible to achieve optimal absorption of each frequency component of an irregular sea without knowledge of the future wave elevation. The array layout is also sub-optimal in the sense that it cannot physically satisfy the optimum for all wave components simultaneously, nor is it practical for the configuration to adapt as the sea state changes. Despite these limitations, in mixed seas we make progress by first identifying the predominant wave frequency and direction, finding appropriate device and array characteristics for this choice. The resulting arrays are then analysed in the broader context of incident waves of different wave number and heading, in order to evaluate the sensitivity of the optimised configuration to deviations from the principal component of the wave spectrum and changing sea states.

In each problem, we will have five bodies with identical geometry and power take-off, separated by at least four radii (to lower the risk of collisions in practical applications) but at most 20 radii in the x or y direction between consecutively numbered bodies to prevent the array becoming too large. Without loss of generality, the first body will be fixed at the origin to reduce the size of the search space.

Since the aim of this optimisation is ultimately a good engineering solution to the problems, we do not require complete certainty that we have reached the true optimum. Moreover, an exhaustive search through local power maxima would be prohibitively time consuming for large numbers of bodies. These are precisely the circumstances under which Genetic Algorithm (henceforth GA) optimisation routines perform best. Here a collection of solutions 'evolve' towards an optimum by favourable characteristics being selected for at each stage of the procedure. For comparison with this method, we will attempt to use knowledge of the nature of array interactions to design configurations with the prescribed characteristics. This will be called the method of Parabolic Intersection (PI).

Section 2 contains a review of the theory relevant to our analysis, while in sections 3 and 4 we go into more detail regarding the techniques used to create arrays. Following this, the behaviour of the arrays created by these techniques will be analysed under a range of wave frequencies and headings in section 5 before some concluding remarks are given in section 6.

2 Theory and Computation

We present here an outline of the interaction theory used in the power calculations. More details may be found in [5, 6]. The mathematical model of the problem consists of an arrangement of N truncated circular cylinders floating vertically in water of finite, constant depth d. Each is attached via a light rod (or taut tether) to a spring and damper, secured to the sea bed. The cylinders may move independently, constrained to the vertical direction, from their neutrally buoyant rest position. The cylinders are of radius a, draught $d-h$ and mass M, the spring and damper having coefficients δ and γ respectively. Gravitational acceleration is denoted by g with ρ representing fluid density. The array is then subject to progressive incident waves of wave number k (angular frequency ω) making an angle β with the positive x-direction.

The velocity potential of wave fields surrounding each device can be represented by a summation of eigenfunctions multiplied by an appropriate set of complex coefficients. Equivalently we may form the scalar product of a vector of partial waves surrounding each body j and a vector of constants. The vector $\mathbf{a}_j$ will then represent the ambient incident wave coefficients and $\mathbf{A}_j$ will represent the coefficients for the wave field scattered by the device. We may determine in advance how waves will interact with a single device by matching eigenfunction expansions in the manner of Yilmaz [4], thus forming the diffraction transfer matrix $\mathbf{B}_j$ and the radiation characteristics vector $\mathbf{R}_j$. Reinterpreting a wave expansion surrounding body i at body j will require a coordinate transformation matrix $\mathbf{T}_{ij}$. Complex heave amplitude X_j, will be related to its non-dimensional counterpart by $X_j = \frac{ig}{\omega^2}.\widehat{X}_j$ whilst velocity and acceleration of each body will be given by X_j' and X_j'' respectively. Kagemoto and Yue [3] proposed the following scattering equation for each body j, relating incident wave coefficients with their scattered equivalents:

$$\mathbf{A}_j = \mathbf{B}_j \left[\mathbf{a}_j + \sum_{\substack{i=1 \\ i \neq j}}^{N} \mathbf{T}_{ij}^T (\mathbf{A}_i + \widehat{X}_i \mathbf{R}_i) \right] \quad j = 1, \ldots, N \quad (1)$$

The total velocity potential ϕ_j surrounding each body may then be formed in terms of similar known quan-

tities alongside the (as yet undetermined) scattered wave coefficients $\mathbf{A}_j$. The hydrodynamic force on each body may be written in terms of this potential as $F_j^H = i\omega\rho \iint_{S_j} \phi_j \, \mathrm{d}S$ where S_j is the under surface of body j. Other forces include the buoyancy force $F_j^B = -\rho\pi a^2 X_j g$ and the force exerted on the body by the power-take off $F_j^G = -\gamma X_j' - \delta X_j$. We may now write the equations of motion for each body using Newton's Second Law:

$$MX_j'' = F_j^H + F_j^B + F_j^G \tag{2}$$

In the case of neutral buoyancy at rest, the mass may be eliminated using $M = \rho\pi a^2(d-h)$. We may then solve these sets of equations simultaneously to yield the scattered wave coefficients and the heave amplitudes. Finally, the power extracted over one wave period T is then

$$P_j = \frac{1}{T}\int_0^T \mathrm{Re}\{F_j^H \mathrm{e}^{-i\omega t}\}\mathrm{Re}\{X_j' \mathrm{e}^{-i\omega t}\}\mathrm{d}t \tag{3}$$

The effect of the array configuration may be more easily understood by forming the *gain*- or $\bar{q}$-factor as the ratio of total power to that of the same number of devices in isolation:

$$\bar{q}^{(\delta,\gamma)}(k,\beta) = \frac{\sum_{j=1}^N P_j^{(\delta,\gamma)}(k,\beta)}{N \times P_0^{(\delta,\gamma)}(k,\beta)} \tag{4}$$

Here, P_0 represents the power from an isolated converter. Also, the superscript (δ,γ) makes explicit the values of spring and damping used in every device but will be subsequently omitted where no confusion is caused. Note that this is distinct from the commonly used q-factor:

$$q(k,\beta) = \frac{\max\limits_{\substack{\delta_1\ldots\delta_N,\\ \gamma_1\ldots\gamma_N}} \left\{\sum_{j=1}^N P_j^{(\delta_j,\gamma_j)}(k,\beta)\right\}}{N \times \max\limits_{\delta_0,\gamma_0}\left\{P_0^{(\delta_0,\gamma_0)}(k,\beta)\right\}} \tag{5}$$

where the isolated and total power expressions have been maximised at every wave number and heading with respect to the spring and damping constants of each individual device (δ_j, γ_j, $j = 0\ldots N$). Fitzgerald and Thomas derived the following consistency condition on the variation of q with β, under the assumptions of point absorber theory [1]:

$$\frac{1}{2\pi}\int_0^{2\pi} q(\beta)\mathrm{d}\beta = 1 \tag{6}$$

Whilst we will use neither the point absorber theory nor optimised individual power take-off characteristics, it will be instructive to form the following consistency constant:

$$c = \frac{1}{2\pi}\int_0^{2\pi} \bar{q}(\beta)\mathrm{d}\beta \tag{7}$$

In order to reactively tune the devices to a given wave frequency, we use the following equations for the spring and damping constants [7] and apply the same values to each generator at all other frequencies:

$$\delta = \omega_0^2(M + m_{33}) - \rho g\pi a^2 \tag{8}$$

$$\gamma = b_{33} \tag{9}$$

Here, ω_0 is the desired tuning frequency, m_{33} is the heave added mass and b_{33} the added damping coefficient. Alternatively, we may employ real tuning of the device by choosing only the damping constant to be non-zero [7]:

$$\delta = 0 \tag{10}$$

$$\gamma = \left[b_{33}^2 + \omega_0^2\left(M + a_{33} - \frac{\delta + \rho g\pi a^2}{\omega_0^2}\right)^2\right]^{\frac{1}{2}} \tag{11}$$

We choose the device to be of radius $a = 1$, draught $d - h = 1$ and the water to have depth $d = 8$, in order to emulate the behaviour of a $5m$ buoy in a water depth of $40m$. Choosing the device tuning frequency to be $2ak = 0.8$ at tuning angle $\beta = 0$ means that peak device power production will coincide with the peak of a JONSWAP spectrum of mean period $5.9s$ [7]. This gives rise to the spring and damping coefficients shown in Table 1.

	$\delta/(\rho a^3\omega_0)$	$\gamma/(\rho a^3\omega_0^2)$
Reactive Tuning	-2.91	0.468
Real Tuning	0	2.94

Table 1: Generator constants.

Although this method is 'exact', numerical implementation requires truncation of an infinite sum of eigenfunctions. Thirty-four vertical modes and nine angular modes were found to be sufficient to calculate the heave amplitudes to an estimated accuracy of 0.5% [6]. However, thirty-three angular modes were needed to give the wave field plots a satisfactory appearance at all points of the domain.

3 Genetic Algorithm

Genetic Algorithms are optimisation routines that are particularly suited: for problems that would take a long time to solve using conventional techniques; for problems where a global rather than a local maximum/minimum is required; where little is known about the function used to evaluate optimality; where it is not essential to obtain the absolute optimum. GAs take their inspiration from the theory of evolution, beginning with a collection of solutions ('population' of 'individuals') and proceeding through a number of generations, the solutions changing at each stage. The best individuals, as evaluated by the user supplied 'fitness function,' will either undergo a random alteration to their defining variables ('mutation' of the 'genotype'), exchange parameters with other highly rated individuals ('crossover'), or will pass on to the next generation unaltered ('elitism'). The least fit individuals at each stage will be removed from the population, and so after many generations only the fittest solutions remain, and the fittest of those is then the output of the optimisation. There are many different variations on this concept and a large range of parameters associated with their use, each of which may lead to better or worse convergence.

In the current application, the individuals are array configurations and their fitness is assessed using the interaction technique outlined in the previous section. The

optimisations were performed using the MATLAB Genetic Algorithm and Direct Search Toolbox [8], with the 'linear feasible' population creation function, 'adaptive feasible' mutation, 'heuristic' crossover, a population size of 30 and 30 generations. It is important to realise that the process involves an element of randomness, so the procedure does not guarantee the same solution every time it is run. We have therefore executed the process 25 times and chosen the best solution from the available results, accepting that it may not be truly optimal. Arrays representing solutions to problems 1, 2 and 3 using this optimisation procedure are shown in Figs. 1 (a), (c) and (e), labelled G1, G2 and G3 respectively.

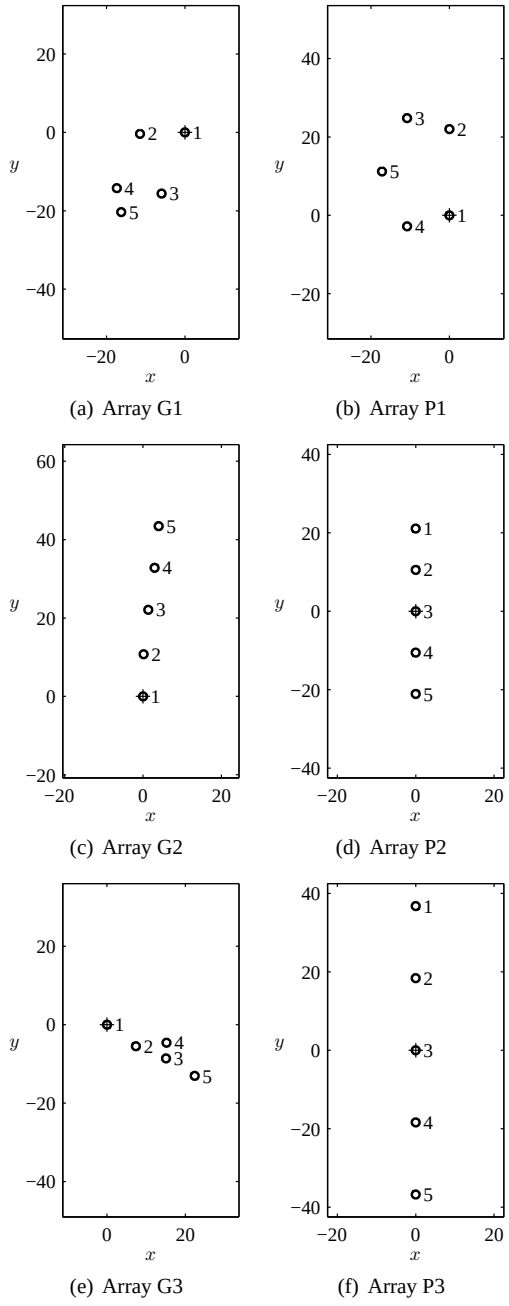

Figure 1: Array configurations.

4 Parabolic Intersection

This method of seeking optimal formations involves a combination of logic and conjecture. The aim is to provide viable solution candidates that satisfy the declared objectives without doing lengthy calculations. We will make some (quite strong) assumptions about the nature of hydrodynamic interactions in order to construct the array and later to interpret selected results. Note, however, that the actual calculation of final array behaviour will be done in full throughout.

The way that the arrays will be constructed involves analysing the wave field around each body in turn. The first assumption is that the wave field resulting from interference between devices is small in magnitude compared with that of the ambient incident wave field. This permits approximation of the full wave field surrounding any element of an array with that surrounding an isolated body. We then identify the progressive part of either radiated or scattered waves as the principal cause of interference and neglect the remaining components. The main areas of constructive and destructive interference relative to the body will then be given by the locations where the interacting wave field is in or out of phase with the ambient incident wave field, as shown respectively by the thick and thin lines of Fig. 2(a) for scattered waves and Fig. 2(c) for radiated waves. Since these plots show the relative phases between two quantities that are both oscillating with the same angular frequency, their values are constant over time, meaning that areas of constructive interference will remain as such and vice-versa. The curves consisting of points with zero relative phase approximately form a family of parabolas, centred on the device.

In order to benefit from the areas of increased wave amplitude surrounding the first device, we then position a second nearby on one of the curves of positive interference. Superimposing a similar set of curves around the second device on to the original pattern highlights the intersections between the families of parabolas as the locations where most positive interference is likely. Thus we may place devices at any of these points and repeat until the array has been constructed. Clearly, there is an element of choice in this process, so a strategy for assembly is needed.

Since the array tuning frequency coincides with the resonant frequency of the reactively tuned devices, motions are large and so radiated waves dominate. The amplitude of these waves diminishes over distance evenly around the device, as shown in Fig. 2(d) for a real tuned converter. Therefore the strongest interference will be found as close as possible to the original device. Furthermore, we can take advantage of mutual positive interaction by placing the devices side-by-side, facing the waves so that they each lie on a parabola surrounding the other body. This can then be repeated to form an equally spaced row, normal to wave incidence as shown by the P2 layout in Fig. 1(d). The same theory can be applied to destructive interference, with the curves defined by

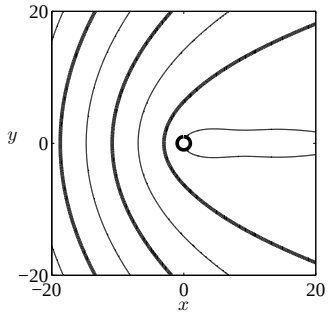

(a) Relative phase between ambient and scattered wave fields. Thick lines: In phase; Thin lines: Out of phase.

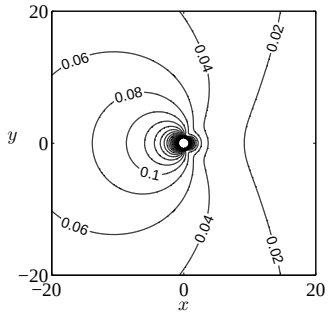

(b) Amplitude of scattered wave field, normalised by ambient wave amplitude. Contours not labelled for values greater than 0.1

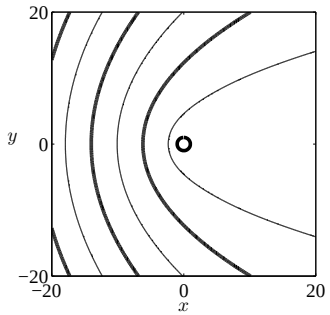

(c) Relative phase between ambient and radiated wave fields. Thick lines: In phase; Thin lines: Out of phase.

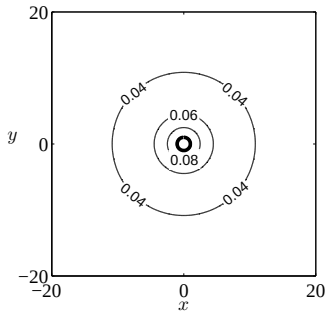

(d) Amplitude of radiated wave field, normalised by ambient wave amplitude.

Figure 2: Radiated and scattered wave field from a real tuned isolated device for $2ak = 0.8$, $\beta = 0$.

points where ambient and interaction-based waves are out of phase. This is the manner in which P3, shown in Fig. 1(f), was constructed.

For the real tuned devices, whose resonant frequency is at $2ak \simeq 1.2$, scattered waves dominate at the array tuning frequency of $2ak = 0.8$. The spatial variation of scattered wave amplitude (shown in Fig. 2(b)) is more complex than for radiated waves, although in general the more valuable interactions are to be gained up-wave of the original device. Starting off as before with a pair of mutually interacting devices side-by-side, we therefore place two more devices in front of the existing two on the intersections of the second and third parabolas away from each body. The fifth body is then placed on the intersection of the second parabolas surrounding the third and fourth bodies. Hence we have designed the array P1 shown in Fig. 1(b) to exhibit several instances of strong up-wave interactions.

5 Results and Discussion

The phase of the scattered wave field relative to the ambient incident wave field for arrays of real tuned devices is depicted in Fig. 3, with a separate plot for interaction with each body (highlighted by a thick circle). Figs. 4 and 5 show the power and heave amplitude resulting from arrays solving problem 3. Finally, the gain factor from all of the arrays is plotted as a function of wave number (Fig. 6) and wave heading (Fig. 7).

5.1 Maximal Array of Real Tuned Devices

The interference patterns from waves scattered by G1 and P1, shown in Fig. 3, are derived from the full calculation (not just overlaid potentials for an isolated body) so the coordinate transformation matrix insists that only points within the distance from each body to its nearest neighbour are valid. The arrays created using the GA and PI methods both exhibit positive interference from the rear cylinders at the up-wave bodies as expected. In fact, many of the bodies in G1 as well as P1 occur at the intersection of positive interference from two or more down-wave bodies.

Array P1 (constructed neglecting radiation) resembles the array with the highest q-factor presented by Fitzgerald and Thomas [1], array S5A, even though the former was assembled under the assumption that scattered waves have the greater magnitude and the latter that radiated waves dominate. However, since both processes form similar parabolic patterns of wave interference (as shown in Figs. 2(a) and 2(c)), an array possessing a similar form to S5A may be constructed in the manner of P1, using radiated instead of scattered waves.

Notice from Fig. 6(a) that array G1 gives a higher value of $\bar{q}$-factor (1.16) at the array tuning frequency and angle than P1 (1.11). This demonstrates that whilst the simplified theory of the parabolic intersection method produces adequate competitors for the GA, there are some factors that contribute to array performance that cannot be easily understood by these means alone.

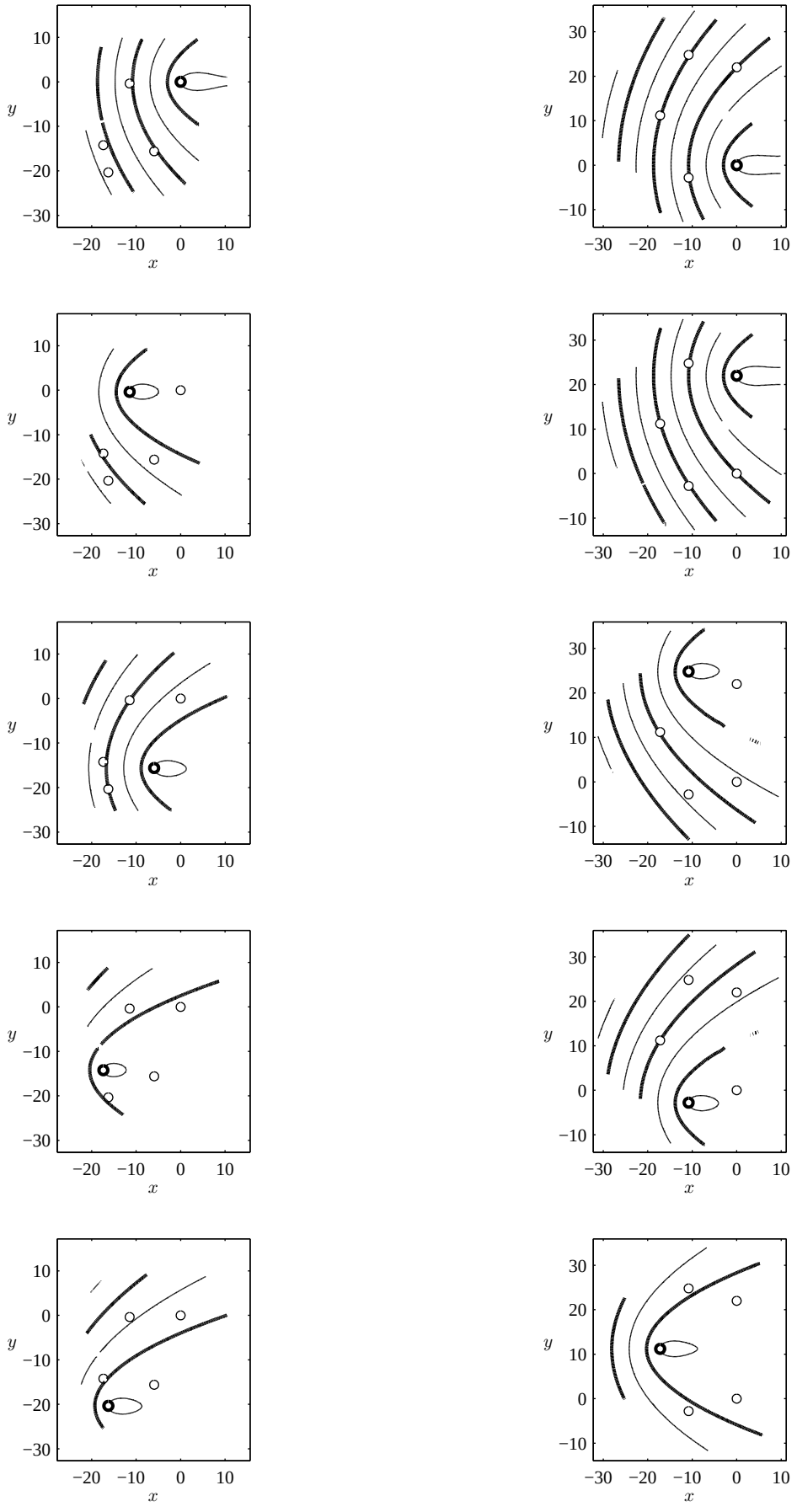

(a) Array G1 (b) Array P1

Figure 3: Relative phase between ambient and scattered wave fields from each member of array (highlighted by thick circle) for $2ak = 0.8$, $\beta = 0$. Thick lines: In phase; Thin lines: Out of phase.

5.2 Maximal Array of Reactively Tuned Devices

There is a striking resemblance between the arrays P2 and G2, generated by the two optimisation methods here. Apart from being essentially a linear array, normal to the incident waves, the mean difference in *y*-coordinates between adjacent bodies is very similar (10.9 for G2 and 10.6 for P2). One should not assume, however, that G2 is an imperfect version of P2. In fact, at the device tuning frequency and angle, G2 marginally outperforms P2 by a $\bar{q}$-factor of 1.77 to 1.71. Despite the similarities in array layout, the behaviour of these two arrays for higher frequencies is completely different. The $\bar{q}$-factor for P2 is dominated by regular, large oscillations due to simultaneous scattering and (to a lesser extent) radiation interference events at all five bodies. Whereas at lower frequencies the GA array is regular enough to take advantage of coordinated radiation interference, higher up the frequency range, the interference patterns become too fine compared with the array irregularities and so analogous simultaneous interaction cannot occur. Hence we see weaker variations in $\bar{q}$-factor at higher frequencies for G2 compared with P2. Returning to the array tuning frequency and varying angle of attack, the similarities between the two arrays overshadow their differences once again and the plots (Fig. 7(b)) are very alike.

5.3 Minimal Array of Reactively Tuned Devices

Four out of the five devices in array G3 appear approximately in a line at such an angle to the incident waves that many of the devices are caught in the broad tail of negative interference from scattering and radiation originating at an up-wave body. This means that the $\bar{q}$-factor is considerably diminished at the array tuning frequency, achieving just $\bar{q} = 0.36$ (Fig 6(c)). The down-wave portion of the interference pattern is the slowest to change shape with wave number and is also very broad, meaning that it encompasses most of the other devices even under large variations in wave number and heading. As a result, the array suffers from poor power output for a considerable portion of parameter space around the tuning frequency and angle without recovering significantly elsewhere. Array P3 results in a lesser reduction in power at the array tuning frequency, yielding $\bar{q} = 0.73$, but the variation with $2ak$ exhibits a much more localised minimum. This means that instead of displaying one peak (as for *N* isolated devices) the total power curve for P3 in Fig. 4 now has two secondary peaks, each expanding the range of wave numbers around the device tuning frequency that enjoy a significant power output. The body heave amplitudes (Fig. 5) also show some reduction at the resonant frequency but not enough to be able to confidently neglect concerns about the small amplitude assumptions of linear wave theory. Just as small changes in wave number lead to a sharp increase in $\bar{q}$-factor for this array, so too does a small change in β (Fig. 7(c)).

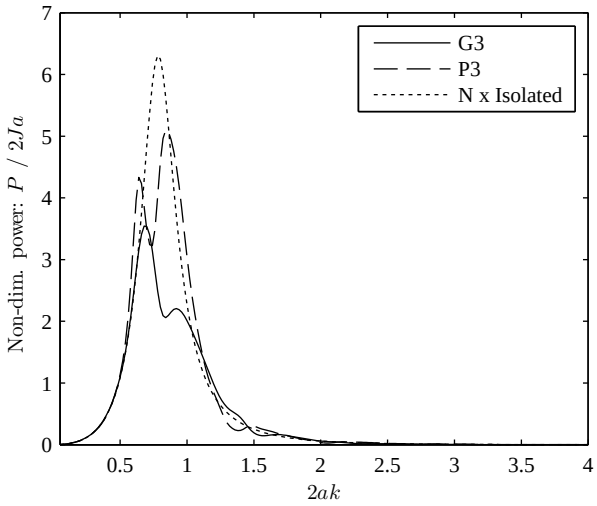

Figure 4: Variation of power with wave number for arrays of reactively tuned devices, minimising power output at desired frequency. Power is non-dimensionalised by the energy contained in a wave of width equal to one device ($2Ja$).

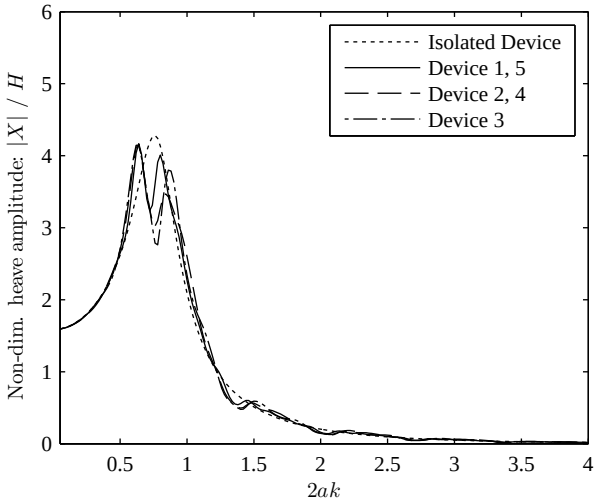

Figure 5: Variation of heave amplitude with wave number for array P3 of reactively tuned devices, minimising power output at desired frequency. Plots 1&5 and 2&4 are the same by array symmetry.

5.4 General Remarks

Reactively tuning the devices ensures greater motion amplitudes near their device tuning frequency of $2ak = 0.8$. We therefore have stronger interactions from radiated waves, so it is no surprise that as β varies, the range of $\bar{q}$-factor values is larger around this frequency for arrays P2/3, G2/3, than for P1 and G1 (Fig. 6).

Whereas the GA produces local maxima/minima at (or very close to) the tuning frequency and angle, those produced using the PI method exhibit stationary points further from the desired parameters. For example, at zero degree wave heading G3 gives rise to a local minimum at $2ak = 0.82$, whereas the corresponding trough for P3 occurs at 0.74 (Fig. 6(c)). It should be noted that in general a local maximum/minimum with respect to

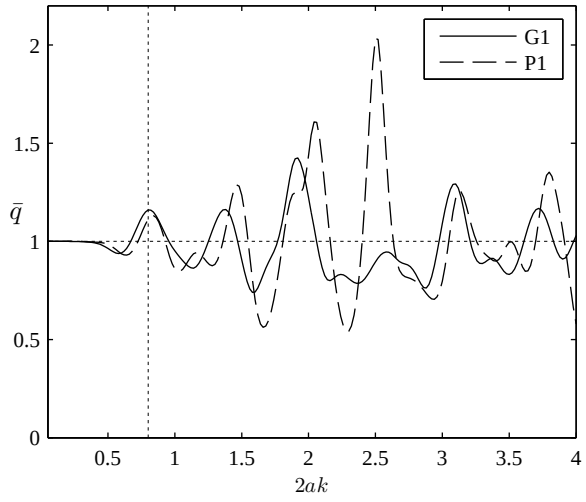

(a) G1 & P1

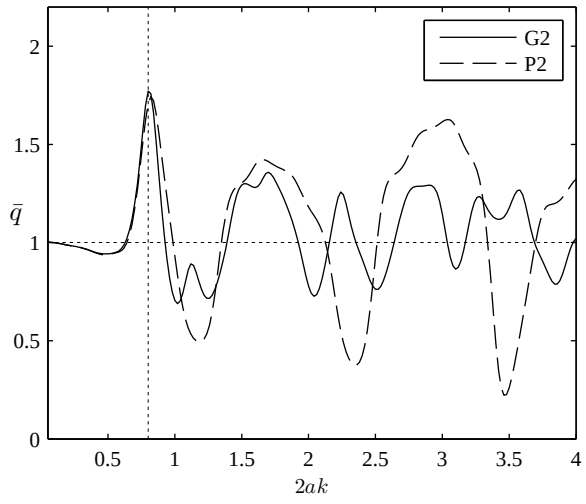

(b) G2 & P2

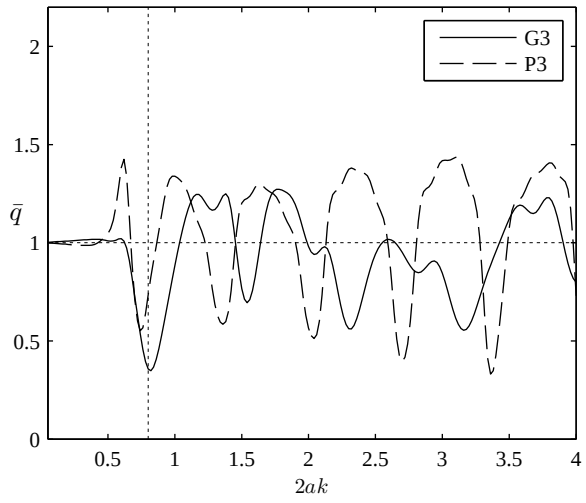

(c) G3 & P3

Figure 6: Variation of gain factor $\bar{q}$ with wave number for arrays of (a) real tuned devices, (b) reactively tuned devices, maximising power output at desired frequency, (c) reactively tuned devices, minimising power output at desired frequency. Wave heading $\beta = 0$ is fixed and the desired frequency ($2ak = 0.8$) is shown by the vertical dotted line.

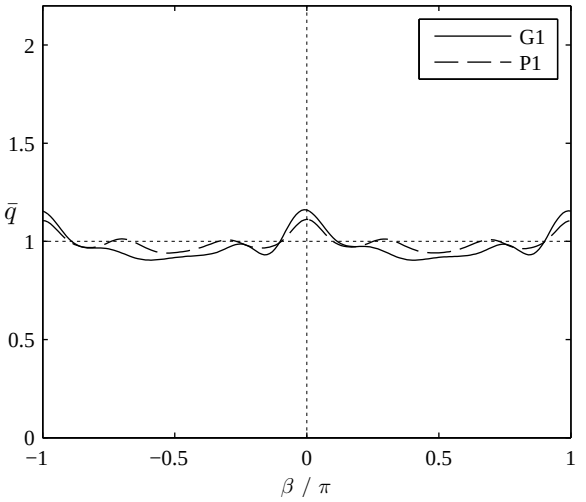

(a) G1 & P1

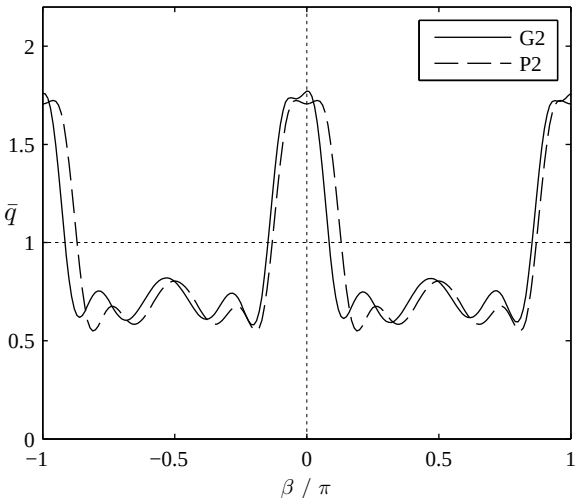

(b) G2 & P2

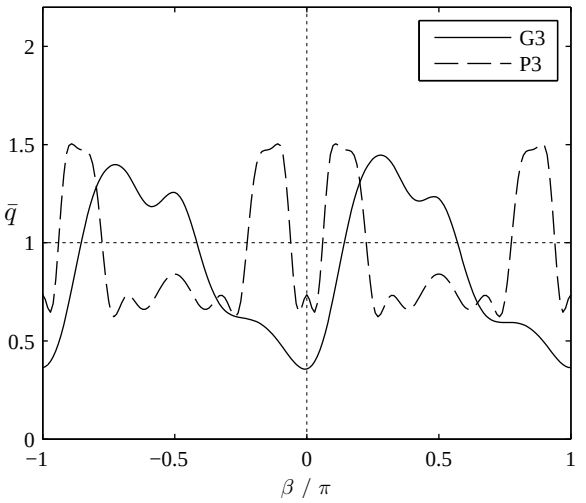

(c) G3 & P3

Figure 7: Variation of gain factor $\bar{q}$ with angle of attack β, for arrays of (a) real tuned devices, (b) reactively tuned devices, maximising power output for desired direction, (c) reactively tuned devices, minimising power output for desired direction. Wave number $2ak = 0.8$ is fixed and the desired direction ($\beta = 0$) is shown by the vertical dotted line.

array configuration does not necessarily imply the same property exists with respect to wave number or angle of attack. However, optimised arrangements will usually exhibit a stationary point in the $\bar{q}$-factor in the immediate vicinity of the tuning frequency, by the following argument. The undulating pattern in the $\bar{q}$-factor plots is due to the interacting waves going in and out of phase with the surrounding wave field at the device locations. Supposing that there is a peak near but not at the tuning frequency and heading, we may try and recreate the associated relative phases at the desired parameters by scaling or rotating the array. If the effect of the resulting changes in wave amplitudes is small compared to that of the phase changes, the peak will be realigned with the tuning frequency, relatively unaltered in shape and size. This will enhance the $\bar{q}$-factor at the tuning parameters, meaning that the original array cannot have been truly optimal. If, however, the peak is already very close to the tuning parameters, the benefit of realigning it at the desired location may be outweighed by its change in magnitude, due to differences in wave amplitudes. Hence, the further away the tuning parameters are from the nearest stationary point, the more we must question the optimality of the array. In the case of the arrays produced with the PI method, any undue loss of performance can be attributed to the simplifying assumptions used in their construction.

Since the consistency condition (6) was derived using point absorber theory with generator characteristics that are individually optimised at each wave number and angle, we do not expect the analogous condition ($c = 1$) to hold in the present circumstance. Nonetheless, for $2ak = 0.8$, there appears to be an approximate balance of positive and negative interference over wave heading angle, as shown by the proximity of the consistency constants (Eqn. (7)) in Table 2 to unity. All of the cases studied result in a value of c lower than 1, particularly for reactively tuned devices (problems 2 and 3). Here, radiated waves dominate, so point absorber theory approximates the exact solution well. Also, since the power of an isolated device has been fully maximised at this frequency, the denominators of the $\bar{q}$-factor (4) and q-factor (5) coincide. Hence the principal difference between the present set of assumptions and those under which the condition was derived is that we do not have the extra facility of individually optimising device characteristics in the array. This explains the discrepancy in consistency constant values for the case of reactively tuned devices. Even if the condition (or worse) does hold, it is not necessarily the case that in mixed seas there will be no gain on average, since we must also take into account the probability of waves arriving from each direction. If the wave headings for which there is beneficial interaction can be adequately aligned with directions of likely wave incidence, favourable power output may still be obtained.

One factor that eases the exploitation of sea state directionality is a large angular tolerance surrounding the target wave heading throughout which the array behaviour is qualitatively the same. The values in Table 2 give the continuous angular range containing the target direction for which $\bar{q} \geq 1$ (for problems 1 and 2) and $\bar{q} \leq 1$ for problem 3. For both maximisation problems, the angular ranges of positive interference are similar, even though the scale of variation is very different. However, the form of the $\bar{q}$-factor plot as we move away from the target wave heading (Figs. 7(a) and 7(b)), is more dome-shaped for arrays P1 and G1 compared with the squarer, double-peaked curve for P2 and G2. Hence power production is comparable with that of the target direction under a larger variation in wave heading for the arrays of reactively tuned devices studied here than for their real tuned equivalents. In the case of array P2, the double peak is a result of the simplifications in the array construction process and the consequent misalignment of what would have been a single peak at $\beta = 0$.

Array	Consistency const [-]	Angular range [deg]
G1	0.98	40
G2	0.90	47
G3	0.88	101
P1	0.99	36
P2	0.90	47
P3	0.94	22

Table 2: Consistency constant, c, as defined by (7) and angular range about $\beta = 0$ for which interaction effects on $\bar{q}$-factor are qualitatively the same. Calculations are for $2ak = 0.8$.

6 Conclusion

Some preliminary examples have been presented of arrays designed to yield modifications in power output. We have demonstrated arrays that, subject to the limitations of linear wave theory, bring about an increase of 77% and a decrease of 64% in the performance of devices under sea conditions for which they were designed to work best. The inclusion of scattered waves in this analysis has allowed consideration of arrays which are closely spaced and whose devices are highly damped. In spite of this, the consistency condition (derived from point absorber theory) still applies reasonably well for the examples studied. We have found that for the device geometry considered, using real tuning of the devices leads to more moderate interactions at the array tuning frequency than for reactively tuned converters and, furthermore, the stability of power output with respect to changing wave heading also depends heavily on this choice.

Results from minimising power at the device tuning frequency have demonstrated that even if we do not seek to increase power, array effects can lead to significantly diminished performance unless care is taken. In terms of broadening the power curve or reducing peak heave amplitude, we found that simply minimising the objective function with the genetic algorithm is probably too crude a method to achieve these aims. The method of

parabolic intersections, however, resulted in reasonable success in these respects.

The GA was found to produce the best arrays purely in terms of their prescribed objective in all cases. We may extract some useful information from the resulting array configurations using simplified analysis, although the configurations do not necessarily reveal all of their beneficial features in such an effortless manner. Despite the strong assumptions adopted, the method of parabolic intersection produced some viable competitors to these arrays with much less computational effort. However, we must accept that the price to pay for the ease of manufacture is that the resulting arrays may not perform as well as those created by more rigorous means.

Further work includes improving the performance of the GA by modifying its input parameters. In particular it may be rewarding to customise how new individuals are created, in order to ensure beneficial array characteristics are passed down through the generations. Naturally, including more generations, increasing the population size or iterating the procedure further are all likely to produce better results. Many more configurations are possible under the PI method of construction, so as more arrays of this type are generated, we may reasonably expect to see further improvements in the performance of the best solutions.

Acknowledgment

The authors would like to acknowledge the support of the EPSRC funded SuperGen Marine Energy Research Consortium.

References

[1] Colm Fitzgerald and Gareth Thomas. A preliminary study on the optimal formation of an array of wave power devices. In *Proceedings of the 7th European Wave and Tidal Energy Conference*, Porto, Portugal, September 2007.

[2] C. J. R. Garrett. Wave forces on a circular dock. *Journal of Fluid Mechanics*, 46(1):129–139, 1971.

[3] Hiroshi Kagemoto and Dick K. P. Yue. Interactions among multiple three-dimensional bodies in water waves: an exact algebraic method. *Journal of Fluid Mechanics*, 166:189–209, 1986.

[4] Oguz Yilmaz. Analytical solutions of the diffraction problem of a group of truncated vertical cylinders. *Ocean Engineering*, 25(6):385–394, 1998.

[5] B. F. M. Child and V. Venugopal. Interaction of waves with an array of floating wave energy devices. In *Proceedings of the 7th European Wave and Tidal Energy Conference, Porto, Portugal*, 2007.

[6] B. F. M. Child and V. Venugopal. Non-optimal tuning of wave energy device arrays. In *2nd International Conference on Ocean Energy (ICOE 2008), Brest, France*, October 2008.

[7] P. McIver, S. Mavrakos, and G. Singh. Wave-power absorption by arrays of devices. In *Proceedings of the Second European Wave Power Conference*, pages 126–133, Lisbon, Portugal, 1996.

[8] MathWorks. Genetic Algorithm and Direct Search Toolbox.